Generalized mean spherical approximations

S. Ciccariello
Dipartimento di Fisica "Galileo Galilei," Università degli Studi di Padova, via F. Marzolo 8, I-35131 Padova, Italy and Sezione di Padova, Istituto Nazionale di Fisica Nucleare, I-35131 Padova, Italy

C. Carraro
California Institute of Technology, M.S. 106-38, Pasadena, California 91125
(Received 21 March 1988)

A criterion for determining the coupling and the exponent [$K(\eta,\beta)$ and $\zeta(\eta,\beta)$] of the one-Yukawa generalized mean spherical approximation (GMSA), which better describes a given real fluid, is suggested. The relative spatial configuration of the surface ($\equiv\Sigma_\chi$) where the compressibility diverges, with respect to the surface ($\equiv\Sigma_\Delta$) bounding the region where physical solutions of the GMSA equations exist, is studied in terms of K, ζ, and η (the packing fraction). Σ_χ is found to lie always in the physically accessible region and to become tangent to Σ_Δ along the η axis; that consequently will be the locus of the critical points of the real systems. By the aforesaid criterion we show that the Baxter solution of the adhesive hard-sphere model can be obtained from the limit of the GMSA solution as $\zeta\to\infty$. The study of the limit $\zeta\to 0$ shows that the GMSA critical indices are generally different from the mean-field ones and that their values depend on the way ζ approaches zero as one moves along the critical isochore and the critical isotherm. Attention is also called to the fact that, as $\zeta\to 0$, $K(\eta,\zeta)/\zeta^2$ has a minimum at $\eta=0.128$, a value rather close to the critical densities of the real fluids.

I. INTRODUCTION

The generalized mean spherical approximation[1,2] (GMSA) of a real fluid consists in approximating the direct correlation function (DCF) by a sum of Yukawa terms in the region external to the core, i.e.,

$$c_{\rm ext}(r,\eta,\beta)\simeq\sum_{n=1}^{N}K_n(\eta,\beta)\exp[-\zeta_n(\eta,\beta)(r-1)]/r\ ,\qquad r>1\ . \quad (1.1)$$

(Here η and β denote, respectively, the packing fraction and the inverse temperature, while the hard-core diameter has been taken equal to 1.) The use of this approximation is quite advantageous for the high degree of analyticity in the resulting expressions of the thermodynamical potentials as well as of the structure functions. However, its practical application in order to predict the thermodynamical behavior of real systems is severely limited by the poor knowledge of $c_{\rm ext}(r,\eta,\beta)$. Following Waisman's original suggestion, recently[3-5] the equations of state of some realistic fluid models, obtained by Monte Carlo (MC) calculations, have been used in order to determine the parameter K and ζ, present on the right-hand side (rhs) of Eq. (1.1) with $N\le 2$. It has turned out that the structural properties, predicted by the resulting GMSA, agree satisfactorily with the corresponding MC ones. This result suggests that the GMSA, even at the level of a single Yukawa contribution, is able to grasp the main physical features of the real fluids, provided K and ζ are chosen to be suitably dependent on η and β. However, the aforesaid analyses dealt with fluids that do not have a critical point;[6] therefore we do not know whether the former conclusion can be extended also to the critical region.

The aim of this paper is to analyze this issue as well as to discuss whether the structure of the region allowed to the GMSA parameters has some relevance with the phase diagrams of the real systems.[2,7,8]

With $N=1$ in Eq. (1.1), the thermodynamical potentials and the structure functions calculated by the GMSA will depend only on η, ζ, and K, henceforth referred to as the natural GMSA parameters. The GMSA equations yield a physically acceptable solution[2,7-13] in a parameter region ($\equiv\mathcal{R}_{\rm GMS}$) more restricted than the one determined by the obvious constraints

$$\zeta>0,\quad 0<\eta<\pi\sqrt{2}/6\ . \quad (1.2)$$

We shall denote by $K=K_\Delta(\eta,\zeta)$ the explicit (local) expression of the surface Σ_Δ, which wraps $\mathcal{R}_{\rm GMS}$. Besides, the GMSA equations predict that the inverse isothermal compressibility is zero on a variety which will be denoted by Σ_χ.

We assume now for a moment that the $c_{\rm ext}(r,\eta,\beta)$ relevant to a real fluid is known. It appears natural to ask the following questions: (a) How can one determine the *best* $K(\eta,\beta)$ and $\zeta(\eta,\beta)$ to be used in Eq. (1.1)? (b) If one lets η and β explore the region physically allowed to the fluid, do the corresponding image points $[\eta,\zeta(\eta,\beta),K(\eta,\beta)]$ always belong to $\mathcal{R}_{\rm GMS}$? (c) Which is

the (η,ζ,K) point representing the critical point (η_c,β_c) of the system in the GMSA natural space? (d) Do the lines representing the coexistence lines of the real fluids lay on Σ_Δ?

In the following we shall try to answer the last three questions after assuming that the answer to the first one is the following? *The best $\zeta(\eta,\beta)$ and $K(\eta,\beta)$ are obtained by requiring that the largest possible number of the next momenta of the Dirichlet*[14,4] *approximation of $c_{\rm ext}(r,\eta,\beta)$, starting from the zeroth one, are equal to the corresponding moments of $c_{\rm ext}(r,\eta,\beta)$.* For our GMSA with $N=1$, this amounts to requiring that

$$K(\eta,\beta)\int_{r>1} r^{2n-1}\exp[-\zeta(\eta,\beta)(r-1)]dv = \int_{r>1} r^{2n}c_{\rm ext}(r,\eta,\beta)dv, \quad n=0,1,\ldots . \tag{1.3}$$

In the following sections we shall work out the consequences of (1.3), which represents the main hypothesis of the paper. Let us try to justify the assumption. We recall the compressibility route to the thermodynamics

$$\beta[\rho\chi_T(\eta,\beta)]^{-1}=\beta\left[\frac{\partial P}{\partial\rho}\right]_T=1-\rho\tilde{c}(0,\eta,\beta)\ , \tag{1.4}$$

where $\chi_T(\eta,\beta)$, ρ, and $\tilde{c}(0,\eta,\beta)$ denote, respectively, the isothermal compressibility, the number density, and the Fourier transform (FT) of the DCF evaluated at zero momentum transfer or, equivalently, the zeroth momentum of the DCF. Starting from the decomposition

$$c(r,\eta,\beta)=c_{\rm int}(r,\eta,\beta)+c_{\rm ext}(r,\eta,\beta)\ , \tag{1.5}$$

where the supports of $c_{\rm int}$ and of $c_{\rm ext}$ are, respectively, the regions $r<1$ and $r>1$, the GMSA is able to reconstruct $c_{\rm int}$ from $c_{\rm ext}$, when this is a sum of Yukawa terms. From Eq. (1.5), the zeroth momentum of the DCF is the sum of the corresponding momenta of $c_{\rm int}$ and $c_{\rm ext}$. The condition (1.3) with $n=0$ assures that, outside the core, the Yukawa approximation has the same momentum of $c_{\rm ext}$. Then, by Eqs. (1.4) and (1.5) the thermodynamics will be exactly reproduced if the $c_{\rm int}$, obtained by solving the GMSA, has the same momentum of the exact $c_{\rm int}$. Of course, generally this will not happen. However, due to the boundedness of the support and to the continuity of the $c_{\rm int}$ resulting from the GMSA, one can reasonably expect that the GMSA $\tilde{c}_{\rm int}(0,\eta,\beta)$ be, in general, rather close to the exact value. Clearly, if we require in Eq. (1.3) the equality of the next-higher-order momenta up to the highest possible order ($\equiv M$), the resulting Dirichlet expression of $c_{\rm ext}$ will have a FT whose McLaurin expansion, truncated at the Mth order, will be equal to that of $\tilde{c}_{\rm ext}(h,\eta,\beta)$. By the same argument invoked above, it is reasonable to expect that the $\tilde{c}_{\rm int}(h,\eta,\beta)$, resulting from the GMSA, be almost exact up to terms $O(h^M)$. This greater accuracy, by duality, will then reflect in a more accurate description of the radial distribution function at larger distances.

The previous discussion represents the main justification of assumption (1.3). In the following we shall analyze some of its consequences. The results and some analogies, that will be noted later, give further support to the assumption. We note that (1.3) represents the key which allows us to associate to a given fluid in the particular thermodynamical state η,β the corresponding point η,ζ,K in the natural GMSA space through the relations

$$\zeta=\zeta(\eta,\beta)\ , \tag{1.6a}$$

$$K=K(\eta,\beta)\ . \tag{1.6b}$$

These questions show that each real fluid is characterized by a particular surface in the GMSA space. In fact, solving Eq. (1.6a) with respect to β and substituting the result in Eq. (1.6b), one gets

$$K=K(\eta,\zeta)\ , \tag{1.7a}$$

$$\beta=\beta(\eta,\zeta)\ . \tag{1.7b}$$

The first equation defines, in the GMSA natural space, the geometrical surface which is made up of all the thermodynamical states of a *class* of fluids, while the second equation singles out the behavior of a particular fluid. In fact, Eq. (1.7b) defines, so to speak, the internal structure of the surface (1.7a) by assigning on it the isotherms characteristic of a particular fluid belonging to the class determined by the considered $K(\eta,\zeta)$ variety. (See Fig. 1). Clearly the interparticle potentials of the fluids forming a particular class may have different functional expressions. However, for a set of fluids obeying a particular law of corresponding states,[15] we shall find that the set is contained in a class. Moreover, since the peculiarities of each fluid belonging to the set are accounted for by an appropriate rescaling of the thermodynamical variables, both Eqs. (1.7a) and (1.7b) are the same for each fluid of the set.

From this discussion it is clear that the analysis of the structure of the region $\mathcal{R}_{\rm GMS}$ will yield restrictions concerning only the varieties $K(\eta,\zeta)$. From our analysis it will turn out that the restrictions are particularly predictive in the two limiting regions $\zeta\to 0$ and $\zeta\to\infty$. For this reason, most of the subsequent discussion is devoted to the analysis of these limits. In fact, we shall show that the critical points have to lie on the η axis while the Baxter[16] solution of the adhesive hard sphere (AHS) model corresponds to a suitable limit of the GMSA solution as $\zeta\to\infty$.

A brief outline of the paper is the following. In Secs. II and III, we briefly sketch Baxter's derivation of the Percus-Yevick solution of the AHS model (Sec. II) and the Høye and Blum[11] derivation of the GMSA equations (Sec. III). In this way, besides emphasizing some aspects which will be later discussed, all the mathematical expressions required in the subsequent analysis will have been explicitly written down, so as to make the paper self-complete and its reading easier. The original results of the paper are discussed in Secs. IV and V. The former is devoted to the analysis of the characteristic GMSA surfaces and to the study of their behavior at small and at large ζ, while the latter (Sec. V) is divided into two parts. In the first we discuss the critical behavior, while in the second we show how the Baxter solution can be obtained from the GMSA solution. A conclusion, Sec. VI, summarizes the main results while four appendixes report some intermediate algebraic expressions.

II. THE AHS MODEL

The adhesive hard-sphere model is obtained from the square-well model

$$\phi(r)/kT \equiv u(r) = +\infty, \quad r<1$$
$$= -\ln[\alpha/12\tau(\alpha-1)], \quad 1<r<\alpha$$
$$= 0, \quad \alpha<r \tag{2.1}$$

by taking the limit $\alpha \to 1^+$ at fixed τ, which can be identified with the temperature.

Baxter obtained the explicit solution of the Percus-Yevick (PY) approximation of this model. This approximation amounts to assuming that

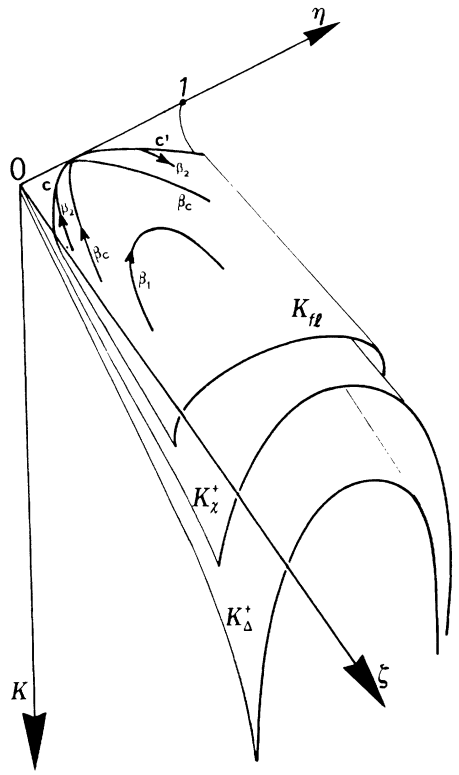

FIG. 1. A schematic picture of the configuration of the surfaces K_Δ^+ and K_χ^+ is reported. No physically acceptable solution can exist below K_Δ^+, which is the lowest surface in the figure. Note that for greater clarity we have chosen the positive direction of the K axis pointing downward. For this reason the surface K_χ^+, where the isothermal compressibility diverges, appears to lie above K_Δ^+. Finally, the third surface depicts the $K(\eta,\zeta)$ variety associated to a class of fluids, while the solid lines illustrate the isotherms relevant to a particular fluid. One should note that the critical point of the fluid corresponds to the point on the η axis, which is the tangency point for the three surfaces. At temperatures smaller than the critical one, the isotherms will have the schematic shape of the curve β_2. This ends on the curve c and reappears on the right from the curve c'. In this way, c and c' represent the coexistence lines of the fluid in the GMSA natural space.

$$c(r,\rho,\beta) \simeq c^{(\mathrm{PY})}(r,\rho,\beta)$$
$$\equiv \{1-\exp[u(r)]\} g(r,\rho,\beta) , \tag{2.2}$$

where ρ denotes the dimensionless density. From Eq. (2.1) it appears evident that $c_{\mathrm{ext}}(r,\rho,\beta)$ can be different from zero only in the interval $[1,\alpha]$, which shrinks to a point in the limit defining the AHS model. This limit requires that the Mayer f bond be

$$f(r) = -1+(1/12\tau)\delta(r-1), \quad 0 \le r \le 1$$
$$= 0, \quad 1<r . \tag{2.3}$$

Then one concludes that $c_{\mathrm{ext}}(r,\rho,\beta)$ is proportional to $\delta(r-1)$. In order to find the exact expression of $c_{\mathrm{ext}}(r,\rho,\beta)$, we recall that the PY approximation neglects the contributions due to the parallel and to the bridge graphs. Thus one gets

$$g(r) = 1+h(r) = [1+f(r)][1+N(r)] , \tag{2.4a}$$

$$c(r) = f(r)[1+N(r)] , \tag{2.4b}$$

$$N(r) = h(r)-c(r) , \tag{2.4c}$$

where $N(r)$, the sum of the nodal graphs, has to be continuous at $r=1$. Let us now put

$$N(1) = -1+\lambda(\rho,\beta)\tau , \tag{2.5}$$

where the moment λ is an unknown function of the density ρ and of the temperature. From Eqs. (2.4b), (2.3), and (2.5) one finds that

$$c_{\mathrm{ext}}(r,\rho,\beta) = (1/12\tau)\delta(r-1)[1+N(1)]$$
$$= (\lambda/12)\delta(r-1) , \tag{2.6}$$

while from Eq. (2.4a) it turns out that

$$h(r) = -1+(\lambda/12)\delta(r-1), \quad r \le 1 \tag{2.7}$$

and thus the cancellation of δ-like contributions on the right-hand side of Eq. (2.4c) is assured.

As Baxter[16] has shown, the solution of the aforesaid model is obtained through the following steps. First, one introduces the function $\tilde{Q}(k)$ as the solution of the equation

$$\tilde{Q}(k)\tilde{Q}(-k) = 1-\rho\tilde{c}(k,\rho,\beta) , \tag{2.8}$$

where

$$\tilde{c}(k,\rho,\beta) = \int \exp(i\mathbf{k}\cdot\mathbf{r}) c(r,\rho,\beta) dv .$$

Baxter proved that, when $c(r)$ has a finite range α,

$$\tilde{Q}(k) = 1-2\pi\rho\int_0^\infty \exp(ikr) Q(r) dr , \tag{2.8a}$$

where $Q(r)$ is real and continuous throughout $[0,\infty]$ and it vanishes identically in $[\alpha,\infty]$. Moreover, he showed that the Ornstein-Zernike (OZ) equation can be converted into the following set of equations:

$$rc(r) = -Q'(r)+2\pi\rho\int_r^\alpha Q'(t)Q(t-r)dt, \quad 0 \le r \le \alpha ,$$
$$rh(r) = -Q'(r)+2\pi\rho\int_0^\alpha (r-t)h(|t-r|)Q(t)dt . \tag{2.9}$$

For the PY approximation of the AHS model, Eq. (2.9) can be explicitly solved by using Eqs. (2.7) and (2.4c) and the continuity properties of $Q(r)$. One obtains

$$Q(r)=a(r^2-1)/2+b(r-1)+\lambda/12, \quad 0<r<1 , \tag{2.10}$$

$$a=\{1+\eta[2-\lambda(1-\eta)]\}/(1-\eta)^2 , \tag{2.11a}$$

$$b=-\eta[3-\lambda(1-\eta)]/2(1-\eta)^2 , \tag{2.11b}$$

and

$$\lambda=6(\tau(1-\eta)+\eta - \{[\tau(1-\eta)+\eta]^2-\eta(2+\eta)/6\}^{1/2})/\eta , \tag{2.12}$$

where $\eta=\pi\rho/6$ is the packing fraction.

III. GMSA

Following very closely the paper by Høye and Blum,[11] we report the main GMSA equations. These authors have shown that in the GMSA case one can still use Baxter's formulation, i.e., Eq. (2.9), although the external DCF is no more identically null beyond α. In fact, they showed that, when the external DCF is a linear combination of Yukawa terms

$$c_{\text{ext}}(r,\rho,\beta)=\sum_{i=1}^{N} K_i \exp[-\zeta_i(r-1)]/r , \tag{3.1}$$

$Q(r)$ obeys Eq. (2.9) with $\alpha=\infty$ and has the following form:

$$Q(r)=\theta(1-r)Q_0(r)+\sum_{i=1}^{N} d_i \exp[-\zeta_i(r-1)] , \tag{3.2}$$

with

$$Q_0(r)=a(r^2-1)/2+b(r-1) + \sum_{i=1}^{N} c_i\{\exp[-\zeta_i(r-1)]-1\} . \tag{3.3}$$

The unknown parameters a, b, c_i, and d_i are determined by solving a set of algebraic equations. [See Eqs. (25) and (28) of Ref. 11.[17]] When $N=1$, setting

$$\zeta\equiv\zeta_1, \quad \delta\equiv d_1, \quad d\delta=-c_1 , \tag{3.4}$$

the aforesaid set of equations reduces to the following quartic equation in δ (Refs. 11 and 7)

$$36\eta^2\delta^4-X(\eta,\zeta)\delta^3+12\eta K\delta^2-KY(\eta,\zeta)\delta+K^2=0 . \tag{3.5}$$

Once the physical root of Eq. (3.5) has been determined, the unknown quantities d, a, and b are simply determined by the following expressions:

$$d=[(-K+\delta Y)\exp(-\zeta)+E(\eta,\zeta)\delta^2]/F(\eta,\zeta)\delta^2 , \tag{3.6}$$

$$a=a_{\text{PY}}(\eta)-\frac{8b_{\text{PY}}(\eta)\delta\exp(\zeta)}{\zeta}\{(1+2\eta-6\eta/\zeta)[d-1-d(1+\zeta)\exp(-\zeta)]+3\eta d\zeta\exp(-\zeta)\} , \tag{3.7}$$

and

$$b=b_{\text{PY}}(\eta)+\frac{8b_{\text{PY}}(\eta)\delta\exp(\zeta)}{\zeta}\{[3\eta/2+(1-4\eta)/\zeta][d-1-d(1+\zeta)\exp(-\zeta)]-(1-4\eta)d\zeta\exp(-\zeta)/2\} . \tag{3.8}$$

For the definition of E, F, X, Y, a_{PY}, and b_{PY} we refer to Appendix A, while here we recall that the isothermal compressibility χ_T is related to a by

$$\beta(\rho\chi_T)^{-1}=\tilde{Q}^2(0)=a^2 . \tag{3.9}$$

IV. THE GMSA CHARACTERISTIC SURFACES

The previous formulation makes evident that the GMSA admits physically acceptable solutions only in a subset of the (η,ζ,K) space. This region (denoted by $\mathcal{R}_{\text{GMS}}$), in fact, corresponds to the one where Eq. (3.5) admits a physical real solution. This property of the GMSA has been first noticed by Waisman.[2] The subsequent work of many authors[8-13] has yielded a considerable simplification both in the GMSA equations and in the expression of the thermodynamical potentials, even in the case of GMSA's involving more than one Yukawa term. In this paper we shall go one step further. On the one hand, we shall obtain the explicit algebraic expressions both of the surface Σ_Δ and of the surface Σ_χ. [See Eqs. (4.5) and (4.13), respectively.] On the other hand, we shall discuss their relative spatial configuration throughout the physically accessible (η,ζ) plane, with particular care to the small- and large-ζ regions.

A. The null-discriminant surface Σ_Δ

The surface which folds the region $\mathcal{R}_{\text{GMS}}$ is essentially[12] given by the condition

$$\Delta(K,\zeta,\eta)=0 , \tag{4.1}$$

where Δ is the discriminant of Eq. (3.5). With some algebra the latter can be explicitly evaluated. We define

$$x=X/36\eta^2, \quad y=Y/6\eta, \quad \hat{K}=K/6\eta \tag{4.2}$$

and find that

$$\Delta=(\hat{K}^3/27)(-64\hat{K}^2r^2+\hat{K}y_1+y_2)\equiv(\hat{K}^3/27)\Delta_R , \tag{4.3}$$

where

$$r\equiv x-y , \quad y_1\equiv(27r^4+72yr^3+56y^2r^2-32y^3r-16y^4)/4 , \quad y_2\equiv y^3x^3 . \tag{4.4}$$

The nontrivial solutions of Eq. (4.1) are

$$K_{\Delta}^{+}=6\eta\hat{K}_{+}(\eta,\zeta)$$
$$=6\eta[y_1+(y_1^2+256r^2y_2)^{1/2}]/128r^2\ , \tag{4.5a}$$
$$K_{\Delta}^{-}=6\eta\hat{K}_{-}(\eta,\zeta)$$
$$=6\eta[y_1-(y_1^2+256r^2y_2)^{1/2}]/128r^2\ . \tag{4.5b}$$

They coincide when

$$y_1^2+256r^2y_2=0\ . \tag{4.6a}$$

Straightforward, albeit long, algebraic calculations convert (4.6a) into

$$y^8P_8(r/y)=0\ , \tag{4.6b}$$

where

$$P_8(t)\equiv 729t^8+3888t^7+8208t^6$$
$$+6592t^5-24032t^4-5120t^3$$
$$+512t^2+1024t+256\ . \tag{4.6c}$$

It has four real roots, t_i, $i=1,\ldots,4$, which are

$$-3.5720,\quad -0.221\,01,\quad 0.355\,17,\quad 1.1996\ . \tag{4.6d}$$

Then the equations

$$x(\zeta,\eta)-(1+t_i)y(\zeta,\eta)=0,\quad i=1,\ldots,4 \tag{4.7}$$

will determine the boundaries of the region, contained in the physical ζ,η half-strip, where Δ turns out positive. We have found no numerical solutions of Eq. (4.7) in the physical (ζ,η) region numerically accessible. Thus we conclude that the varieties (4.5a) and (4.5b) exist throughout the region $\zeta>0$ and $0\le\eta<1$. Besides, by using the *large-ζ* asymptotic expansions of the quantities X and Y reported in Appendix A [see Eqs. (A11) and (A12)], one finds that

$$K_{\Delta}^{+}\approx 9\zeta^2/512\eta\to+\infty\ , \tag{4.8a}$$
$$K_{\Delta}^{-}\approx-\frac{16}{3}\left[\frac{\eta(2+\eta)}{(1-\eta)^2}\right]^2\zeta^{-4}\to 0^-\ , \tag{4.8b}$$

while, by using the *small-ζ* asymptotic expansions reported in Appendix A [see Eqs. (A16) and (A20)], one finds

$$K_{\Delta}^{+}\approx\zeta^2\frac{a_{\mathrm{PY}}^2}{24\eta}\to 0^+\ , \tag{4.9a}$$
$$K_{\Delta}^{-}\to-\frac{(1+2\eta)^4}{96\eta(1-\eta)^6}\ . \tag{4.9b}$$

From this analysis one concludes that the image of the region physically accessible cannot be larger than the (η,ζ,K) region delimited by the two surfaces (4.5a) and (4.5b). (See Fig. 1.)

B. The infinite-compressibility surface Σ_χ

In order to complete the analysis of the geometrical features of the parameter space (η,ζ,K) we have to determine the surface where the inverse compressibility vanishes, i.e., we have to look for the solution of

$$a(\eta,\zeta,K)=0\ . \tag{4.10}$$

We shall denote by $K_\chi(\eta,\zeta)$ the solution of this equation. Its explicit algebraic expression can be obtained through the following steps. First one solves with respect to d the linear equation obtained by equating to zero the lhs of Eq. (3.7). Then one substitutes the result on the lhs of Eq. (3.6) and one solves the resulting linear equation in K. With the following definitions:

$$A_1(\eta,\zeta)\equiv 2\left[Y-\frac{\zeta a_{\mathrm{PY}}F}{8b_{\mathrm{PY}}F_1(\eta,\zeta)}\right]\ , \tag{4.11a}$$
$$A_2(\eta,\zeta)\equiv 2\left[\frac{EF_1(\eta,\zeta)-f_1(\eta,\zeta)F}{F_1(\eta,\zeta)}\right]\exp(\zeta)\ , \tag{4.11b}$$

where F_1 and f_1 are defined in Appendix A (see Eqs. (A7a) and (A7d)], one gets

$$K=\delta A_1/2+\delta^2A_2/2\ . \tag{4.12}$$

Then one solves Eq. (3.5) with respect to K, and by equating the result to (4.12), one gets an equation in the unknown δ. After eliminating the trivial double solution $\delta=0$, one is left with a quadratic equation whose solutions are

$$\delta_\chi^{\pm}=[-B_1\pm(B_1^2-B_0B_2)]^{1/2}/B_0\ , \tag{4.13}$$

where

$$B_0\equiv(A_2+12\eta)^2\ ,$$
$$B_1\equiv A_2(A_1-Y)+12\eta A_1-2X\ , \tag{4.14}$$
$$B_2\equiv A_1(A_1-2Y)\ .$$

The substitution of (4.13) in (4.12) yields the sought after algebraic expressions of $K_\chi(\eta,\zeta)$. Although these expressions are still rather involved, one can analyze their behavior both at large and at small ζ. In particular, in the former region, by using the asymptotic expressions required in Appendix A [see Eqs. (A11)–(A15)], one finds that the leading term of the discriminant of Eq. (4.13) is

$$[12(1-\eta)\eta\zeta^2/(1+2\eta)]^2$$

and thus it is always positive. Since A_i and B_1 are $O(\zeta)$ while B_0 and B_2 are $O(\zeta^2)$, one concludes that, as $\zeta\to\infty$, the $\delta_\chi^{\pm}$ have finite limits. These are given by Eq. (A15). Then from Eq. (4.12) it follows that $K_\chi^-\approx 0$ while

$$K_\chi^+\approx\frac{1+2\eta}{24\eta(1-\eta)}\zeta+o\ . \tag{4.15}$$

Physically the interesting region is the one where K is the positive and thus we shall be confined to it. One concludes that at very large ζ the surface where the compressibility diverges is below the surface K_Δ^+.

Although the behavior of K_χ^+ at very small ζ can be obtained by analyzing the small-ζ behavior of the roots (4.13), we have directly analyzed the quantity $a(\eta,\zeta,K)$ as ζ and K tend to zero inside the physical region: $0<K\le K_\Delta^+(\eta,\zeta)$. In order to meet this condition we

have analyzed the small-ζ behavior of $a(\eta,\zeta,K)$ by assuming that

$$K \approx \kappa(\eta)\zeta^{\varpi} , \tag{4.16}$$

$$\kappa(\eta) > 0, \quad \varpi \geq 2 . \tag{4.17}$$

One should refer to Appendix B for details on this analysis. The main conclusion is that

$$a = a_{\mathrm{PY}} + O(\zeta) \quad \text{when } \varpi > 2 , \tag{4.18}$$

while

$$a = \frac{48\eta\kappa(\eta) - 2a_{\mathrm{PY}}^2 r_a(\eta)}{2a_{\mathrm{PY}} r_a(\eta)} + a_1(\eta)\zeta + o(\zeta) \quad \text{when } \varpi = 2 , \tag{4.19a}$$

where the later convenience the term $O(\zeta)$ has been written in an explicitly factorized form and

$$r_a(\eta) \equiv 1 - [1 - 24\eta\kappa(\eta)/a_{\mathrm{PY}}^2]^{1/2} . \tag{4.19b}$$

The results (4.18) and (4.19) are particularly interesting. Indeed, (i) If one lets $\kappa(\eta)$ go to zero, one finds that $a \to a_{\mathrm{PY}}$, as one should expect, since in this limit one practically recovers the case $\varpi > 2$. (ii) Expression (4.19b) makes sense only when

$$\kappa(\eta) \leq a_{\mathrm{PY}}^2/24\eta . \tag{4.20}$$

Moreover, when one considers the equality sign in (4.20), one sees that (4.16) becomes equal to (4.9a). In other words, the condition $0 < K \leq K_{\Delta}^{+}(\eta,\zeta)$ implies the validity of (4.20) at very small ζ. (iii) Finally, from Eqs. (3.9), (4.18), and (4.19a), one sees that the inverse compressibility becomes null, i.e., $\chi_T^{-1} = a^2 = 0$ only when

$$\kappa(\eta) = a_{\mathrm{PY}}^2/24\eta \equiv \kappa_0(\eta), \quad \omega = 2 . \tag{4.21}$$

In conclusion, inside the physical parameter region and in the limit $\zeta \to 0$, the surface Σ_{χ} becomes tangent to the surface Σ_{Δ} along the η axis, while $\kappa_0(\eta)$ turns out to be equal to $a_{\mathrm{PY}}^2/24\eta$. Besides, the first surface lies below the second at very small *and* at very large ζ due to the conditions (4.20) and (4.15), respectively. Outside these regions, the relative geometrical configuration of K_{Δ}^{+} and of K_{χ}^{+} has been explored numerically rather thoroughly throughout the physical (η,ζ) half-strip, and we have always found

$$K_{\chi}^{+}(\eta,\zeta) < K_{\Delta}^{+}(\eta,\zeta) .$$

Therefore we conclude that the variety Σ_{χ} lies always below the variety Σ_{Δ},[18] in the positive half-space $K > 0$ (see Figs. 1 and 2).

V. APPLICATIONS

The relative geometrical configuration of Σ_{Δ} and Σ_{χ} is particularly interesting for its consequences on the idea of approximating the external DCF by a single Yukawa term. In fact, we shall discuss two topics: (i) What kind of critical behavior can be obtained by the GMSA and (ii) How Baxter's result on the AHS model fits in the former GMS scheme. It should be noted that the two issues correspond to study the GMSA limits: $\zeta \to 0$ and $\zeta \to \infty$, respectively.

A. Critical behavior

We show now that the GMSA can predict, although in an approximate way, many aspects of the critical behavior of real systems. In order to find out where the critical points have to be located in the natural GMSA space, we recall that in the early 1960's Green[19] pointed out that the HNC approximation of the DCF at the critical point must be long ranged. Subsequent important papers[20] by Fisher and by Polyakov have shown that this is true in general. In fact, they showed that at the critical point the CF for large distances decreases as

$$h(r,\eta_c,\beta_c) \sim \frac{1}{r^{1+\bar{\eta}}} \quad \text{with } \bar{\eta} > 0 , \tag{5.1}$$

with $\bar{\eta}$ positive and depending only on the space dimensionality.[21,22] By Green's argument[19] one deduces that

$$c(r,\eta_c,\beta_c) \sim \frac{1}{r^{5-\bar{\eta}}}, \quad r \gg 1 . \tag{5.2}$$

This behavior implies that in approaching the critical point the zeroth moment of c_{ext} is finite while the second one diverges as $r^{\bar{\eta}}$. According to the criterion (1.3), the

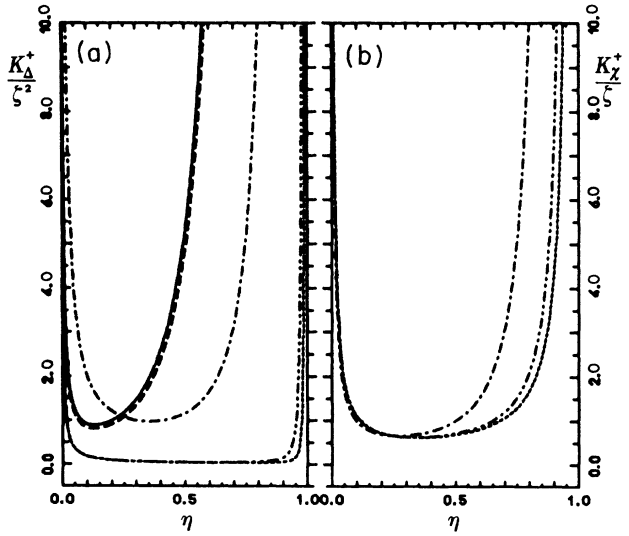

FIG. 2. (a) Sections of the K_{Δ}^{+}/ζ^2 surface, at fixed ζ values, are shown for different ζ values. The curves refer to the values $\zeta = 0.001$ (—); 0.1 (- - -); 10.0 (-·-); 50.0 (-···); 100.0 (· · ·), respectively. We note that (i) on the figure's scale the first two curves also represent K_{χ}^{+}/ζ^2. In fact, a magnification of the scale by a factor of 10^6 is necessary for observing some difference. (ii) For the third curve (the dash-dotted line) the vertical scale must be multiplied by a factor of 10. Consequently, differences with the shape of the corresponding K_{χ}^{+}/ζ curve shown on the right have already become appreciable. (b) The curves show the ζ sections of the surface $K_{\chi}^{+}(\eta,\zeta)/\zeta$ for the three highest ζ values reported before.

best one-Yukawa GMSA must be characterized by the same momenta and thus it is determined by the two following conditions:[23,24]

$$K(\eta,\beta)\simeq\kappa(\eta_c,\beta_c)\zeta^2 , \tag{5.3}$$

$$\zeta\to 0 , \tag{5.4}$$

with

$$\kappa(\eta_c,\beta_c)\simeq\int_1^\infty r^2 c_{\rm ext}(r,\eta_c,\beta_c)dr . \tag{5.5}$$

However, the GMSA resulting from Eqs. (5.3) and (5.4) will describe a critical behavior only if it yields a divergent compressibility. In the second part of Sec. IV we have studied the behavior of $a(\eta,\zeta,K)$ at very small ζ, and we have found that it tends to zero only when

$$\kappa(\eta_c,\beta_c)\approx\kappa_0(\eta_c) . \tag{5.6}$$

In this way $\kappa(\eta,\beta)$ turns out perfectly determined and independent of the temperature. This property, combined with Eq. (5.5), implies that the external DCF's of two different fluids, having different critical temperatures but the same critical packing fraction, have approximately the same zeroth momentum. The present knowledge of the $c_{\rm ext}$'s of the real systems does not allow us to check this result. However, Eq. (5.6) contains further physical information worth pointing out. Using the $a_{\rm PY}$ definition of Eq. (A1a), $\kappa_0(\eta)$ becomes

$$\kappa_0(\eta)=(1+2\eta)^2/24\eta(1-\eta)^4 . \tag{5.6a}$$

The dependence of $\kappa_0(\eta)$ on η implies by Eqs. (5.6) and (5.5) that the overall attractive contribution, accounted for by $c_{\rm ext}$, turns out to be larger both at small and at high densities. This appears physically quite sound. At small densities a large attractive contribution is required in order to compensate for the rather large average distance between particles, while at larger densities the stronger attractive effects are required for overcoming the dominant repulsive ones. From Eq. (5.6a) the smallest effective attractive contribution is found at the packing-fraction value $\eta_0=0.128$. Let us consider the collection of real fluid systems. Since by a suitable rescaling one can always make the diameter of the effective core of each fluid equal to 1, the repulsive forces in the rescaled systems will turn out equal. It is now tempting to assume that the smaller the effective attraction, the higher the probability that the system does physically exist. In this way one would expect that the critical packing fractions of the real fluids are distributed around the value η_0. The results reported in the sixth column of Table I show that this property is reasonably verified although the distribution appears slightly shifted toward the right.

It is known that at the critical point the large-r behavior of $h(r)$ is the same, independent of the particle interaction. Then, from Eq. (5.2), one could write in first approximation

$$c_{\rm ext}\simeq\gamma_p(\beta\varepsilon)/r^{5-\bar\eta},\quad r\geq 1 , \tag{5.7}$$

where the function γ_p is characteristic of the fluid potential and $\beta\varepsilon$ is the dimensionless coupling constant. From this approximate equation and by Eq. (5.5) and (5.6) one obtains

$$\kappa_0(\eta_c)\simeq\gamma_p(\beta_c\varepsilon)/(2-\bar\eta) .$$

In the last two columns of Table I we have reported respectively the values of $\beta_c\varepsilon$ and those of $\kappa_0(\eta_c)$. They are sufficiently close to conclude that $\gamma_p(x)$ is linear in the range $x\simeq 1$.

Having discussed the location of the critical point, for completeness we now have to discuss the critical behavior resulting from the one-Yukawa GMSA. We have already used the property that in approaching the critical point, $\zeta(\eta,\beta)$, the inverse correlation length of the one-Yukawa GMSA of the DCF, must go to zero. Thus it appears natural to assume that

$$\zeta\approx Z_T(\eta_c)\,|\,\varepsilon_T\,|^{\nu_T}+Z_\eta(\eta_c)\,|\,\varepsilon_\eta\,|^{\nu_\eta} , \tag{5.8}$$

where $\varepsilon_T\equiv(T-T_c)/T_c$, $\varepsilon_\eta\equiv(\eta-\eta_c)/\eta_c$, and Z_T and Z_η are positive quantities depending on the particular fluid. Clearly the real positive exponents ν_T and ν_η specify the ways the *second* moment of the DCF diverges as the critical point is approached along the critical isochore or the critical isotherm, respectively. Due to the OZ equation and to the universal behavior of the CF in the critical region, the quantities ν_T and ν_η have to be universal too, as it will appear more clearly later. For these reasons they will be referred to as the *critical indices* of the correlation length of the DCF. By the preceding GMSA analysis one can easily express the well-known critical indices in terms of the former ones. To this aim we recall that, for any fluid, $K_{fl}(\eta,\zeta)$ becomes tangent to K_χ^+ and to K_Δ^+ at the critical point (see Fig. 1). It appears natural to assume that on K_{fl}, a turns out analytic with respect to ζ. Then, from Eq. (4.19a) and by Eq. (4.21), one finds that

$$\beta(\rho\chi_T)^{-1}\approx a_1^2(\eta_c)\zeta^2 . \tag{5.9}$$

The scaling properties of the isothermal compressibility are evident and from Eq. (5.9) it immediately follows that

$$\bar\gamma=2\nu_T,\quad \bar\delta=2\nu_\eta+1 . \tag{5.10}$$

These relations allow us to determine the critical indices of the DCF from the knowledge of the well-known ones. Vice versa, the latter ones can be expressed in terms of the former ones, since we are allowed to take as independent the indices $\bar\delta$ and $\bar\gamma$. We must note, however, a serious limitation of the GMSA's, involving a finite number of Yukawa terms, in describing the critical behavior of the real systems. This shortcoming is essentially related to the fact that the approximation (1.1) is unable to yield the noninteger power-law behavior of the DCF at the critical point, described by Eq. (5.2). In particular, in the case of the one-Yukawa GMSA, one finds that (see Appendix C for details)

$$h(r,\ldots)\sim\zeta^2\frac{\exp[-\,|\,a_1(\eta)\,|\,\zeta^2 r/a_{\rm PY}(1-2\eta)]}{r} ,$$

$$r\gg 1 . \tag{C9}$$

TABLE I. In the fourth and fifth column we report the critical temperature and the critical density relevant to the fluids present in the first column. These values have been taken mostly from the *Handbook of the American Institute of Physics.* The second and third columns report, respectively, the value of the coupling constant (in units of k_B) and that of the characteristic length of the potential. The analytic expression of the latter is the square-well, the Stockmayer, or the (6-12) Lennard-Jones one, depending on whether in the last column one finds, respectively, SW, Stm, or other symbols, respectively. In fact, *V* and η denote that the LJ parameters have been determined by virial or by viscosity measurements, respectively. Besides, in the first rows, the symbol QM specifies that the determination of the LJ parameters has been carried out by the quantum-statistical method. The data inside square brackets refer to the electric dipole moment and are given in Debye units. These data have been mainly taken from Ref. 25. (Actually, in the table we report only the most typical cases, including the ones which lie farther from the minimum.) The sixth column shows the critical packing fraction. In evaluating this quantity we have simply identified the core radius with σ. This fact most likely yields an overestimate of the core for the LJ and for the Stm potentials. One sees that the values are scattered around $\eta_0=0.128$, the most likely GMSA value, although they are more frequent in the higher-density region. Finally, the penultimate and the last column allow us to compare the dimensionless coupling constant with the $\kappa_0(\eta_c)$ value, which should approximate the zero moment of the DCF. Moreover, we note that the value of $\kappa_0(\eta)$ at the most likely density value η_0 is 0.888, a value quite close to the values reported in the last column. This result is mainly a consequence of the shape of $\kappa_0(\eta)$ around the minimum, as one can see from the solid line shown in Fig. 2(a).

Fluid	ε/k_B	σ (Å)	T_c (K)	$\rho_c\left[\frac{g}{cm^3}\right]$	η_c	$\frac{\varepsilon}{k_B T_c}$	$\kappa_0(\eta_c)$	
He	10.22	2.556	5.2	0.0693	0.091	1.96	0.937	QM
H_2	36.7	2.928	32.9	0.0308	0.122	1.12	0.889	QM
Ar	119.8	3.405	150.72	0.5308	0.165	0.795	0.919	*V*
N_2	95.3	3.70	126.26	0.311	0.177	0.755	0.941	*V*
	53.7	3.299			0.147	0.426	0.896	SW
Cl_2	357.0	4.115	417.16	0.573	0.178	0.856	0.943	η
	257.0	4.400			0.217	0.616	1.050	SW
CO_2	189.0	4.486	304.2	0.468	0.303	0.621	1.503	*V*
	205.0	4.07			0.226	0.673	1.083	η
	119.0	3.917			0.201	0.391	0.999	SW
H_2O	380.0[1.83]	2.65	647.4	0.326	0.106	0.587	0.904	Stm
HCl	360.0	3.305	324.55	0.420	0.132	1.109	0.888	η
NH_3	692.0	2.902	406.41	0.235	0.107	0.787	0.993	SW
	320.0[1.47]	2.60			0.077	0.787	0.993	Stm
CCl_4	327.0	5.881	558.3	0.558	0.233	0.586	1.110	*V*
	469.0	4.294			0.091	0.840	0.937	SW
$CHCl_3$	327.0	5.430	536.54	0.496	0.210	0.609	1.027	η
	1060.0[1.05]	2.98			0.035	1.976	0.581	Stm
C_2H_6	243.0	3.954	305.43	0.2056	0.131	0.796	0.888	*V*
	230.0	4.418			0.183	0.753	0.954	η
	244.0	3.535			0.094	0.799	0.928	SW
C_2H_4	199.2	4.523	282.65	0.218	0.227	0.705	1.086	*V*
C_2H_2	185.0	4.221	308.53	0.2308	0.210	0.600	1.027	η
CH_3OH	507.0	3.585	513.2	0.272	0.124	0.901	0.888	η
	630.0[1.66]	2.40			0.037	1.228	1.510	Stm
CS_2	488.0	4.438	552.0	0.441	0.160	0.884	0.911	η

The expression of the denominator would imply that $\bar{\eta}=0$, a mean-field value, but the presence of the factor ζ^2 in the numerator implies that at the critical point the numerator factor is not *finite and different* from zero as the correct scaling requires.[20] The presence of the factor ζ^2 is nothing but a caricatural attempt of the GMSA to reproduce a decrease faster than r^{-1}. Moreover, from Eq. (C9), the inverse correlation length of the CF is characterized by the two indices,

$$\bar{\nu}=2\nu_T, \quad \bar{\nu}_c=2\nu_\eta \ . \tag{5.11}$$

The comparison with Eq. (5.10) yields

$$\bar{\nu}=\bar{\gamma}, \quad \bar{\nu}_c=\bar{\delta}-1 \ . \tag{5.12}$$

The first of the (5.12) relations is not obeyed by the measured critical indices and the observed structure factors do not show the behavior predicted by Eq. (C9). Thus we have to conclude that, as expected, the critical behavior predicted by the GMSA (Ref. 23) is not satisfactory.

B. Baxter's solution of the AHS model

According to Eq. (2.6), this solution requires a δ-like behaved $c_{\rm ext}(r,\eta,\beta)$. By our assumption (1.3), the best GMS approximation of $c_{\rm ext}$ by a single Yukawa term has to reproduce the maximum number of next momenta of (2.6), starting from the lowest one. In this case the momenta of the exact $c_{\rm ext}$ can be exactly and easily calculated and thus Eq. (1.3) yields

$$K_{\rm AHS}\exp(\zeta)\left[-\frac{d}{d\zeta}\right]^{2n+1}\left[\frac{\exp(-\zeta)}{\zeta}\right] = \frac{\lambda(\eta,\tau)}{12}, \quad n=0,1,\ldots \ . \tag{5.13}$$

One sees that all these conditions can be fulfilled, provided

$$\zeta\to\infty \tag{5.14}$$

and

$$K_{\rm AHS}(\eta,\tau)\approx\frac{\lambda(\eta,\tau)}{12}\zeta \ . \tag{5.15}$$

In particular, Eq. (5.14) assures the equality of the ranges of $c_{\rm ext}$ and of its one-Yukawa approximation, while Eq. (5.15) assures that the limit of this approximation is equal to the exact $c_{\rm ext}$ of the PY approximation of the AHS model. In other words, in the case of the Baxter solution of the AHS model, the limit (5.14) and the condition (5.15) guarantee that the Dirichlet approximation of $c_{\rm ext}$ become exactly equal to the latter. Since both the GMSA and Baxter's solution method use the core condition in order to determine the DCF in the region internal to the core, it is clear that the aforesaid limit of the GMSA solution, with the condition (5.15), yields the Baxter solution of the AHS model. Besides, one should also note that Eq. (5.15) already takes into account the exact value of $\lambda(\eta,\tau)$ that Baxter obtained by exploiting the continuity of $N(r,\eta,\beta)$ at the core border.

In order to be sure that no mathematical surprise comes out from the limit procedure, we have directly calculated the limits of the most important quantities. Leaving the details in Appendix D, we have found that

$$a\approx a_{\rm PY}-\frac{\eta(1-\eta)}{(1-\eta)^2}\lambda+O(\zeta^{-1}) \ , \tag{5.16}$$

$$b\approx b_{\rm PY}+\frac{\eta(1-\eta)}{2(1-\eta)^2}\lambda+O(\zeta^{-1}) \ . \tag{5.17}$$

Once we substitute Eq. (2.6) for λ, Eqs. (5.16) and (5.17) coincide with Eqs. (7.31) of Ref. 16. In the same limit, using Eqs. (5.16), (5.17), (D4), and (D5), the equality of the $Q(r)$, defined by Eqs. (3.5) and (3.6), with the corresponding function used by Baxter [see Eq. (7.30) of Ref. 16] is immediate. In this way the proof is complete.

It is interesting to discuss how the phase diagram of the AHS model (see Fig. 12 of Ref. 16) fits into the structure of the $\mathcal{R}_{\rm GMS}$ region. We recall that when the temperature τ becomes smaller than a characteristic value $\tau_c(\equiv 0.0976)$, the Baxter solution does not exist in a range of densities depending on the value of τ. One should note that this lack of solutions is not due to the fact that the trajectory of the $(\eta,\zeta,K_{\rm AHS})$ representative points meets with the surface Σ_Δ as $\zeta\to\infty$. This in fact is not possible, since, as $\zeta\to\infty$, K_Δ^+ increases as ζ^2, see Eq. (4.8a), and thus it lies far above $K_{\rm AHS}(\eta,\zeta)$, which according to Eq. (5.15), increases only linearly.[26] One concludes that the AHS diagram is not determined by the surface Σ_Δ. On the contrary, it is determined by the boundary of the holomorphy domain of the function $\lambda(\eta,\tau)$. In fact, the coexistence line is made up of the branch points of the analytic function (2.12), which, by Eq. (2.5), represents the sum of the nodal graphs of the PY approximation of the AHS model.

Before trying to give a heuristic answer to the question whether the images of the coexistence lines of the real fluids have to lie on Σ_Δ we make some preliminary remarks.

The application of the criterion (1.3) to the one-Yukawa GMSA *generally* yields a unique determination of K and ζ, since one requires the equality of the first two moments. Moreover, far from the critical region one expects that $\zeta\simeq 1$ and that $K\simeq 0$ at sufficiently high temperatures. Thus, in the GMSA natural space, the representative points of the systems in the above specified physical conditions will lay below Σ_χ and thus also below Σ_Δ. Let us imagine now that a fluid, starting from one of these configurations, continuously approaches a point on the coexistence line. If the image of this line lies on Σ_Δ, one of the following possibilities ought to take place. The trajectory of the best image points $(\eta,\zeta(\eta,\beta),K(\eta,\beta))$ is continuous, and thus it crosses Σ_χ or it is discontinuous and thus it avoids the crossing of Σ_χ by making a jump. Due to the nonlinearity of the constraints (1.3), the latter possibility cannot be excluded on purely mathematical grounds, although it appears physically rather odd. The former possibility implies that, in the neighborhood of the point where the trajectory crosses Σ_χ, the GMSA would predict a divergent compressibility and thus it would yield a poor description of the real fluid behavior.

The results of a recent GMSA analysis[4] of the HS fluid do not find any indication of such a behavior. In fact, the trajectory of the first pole of the FT of the total correlation function (CF), $\tilde{h}(z,\rho)$, reported in Fig. 5 of Ref. 4, shows that the compressibility is always far from becoming divergent, while the resulting K and ζ, see Fig. 2 of Ref. 4, depend continuously on the density, even beyond the freezing density.[27] From a practical point of view, the GMSA fluid variety, i.e., Eq. (1.7a), can be determined by Eq. (1.3) only when c_{ext} is known. Consequently, the mapping (1.6) can no longer be defined beyond the coexistence line. If the variety (1.7a) were made up of (at least) two pieces, one above and one below Σ_χ, then the coexistence line could be mapped just at the intersection of the variety (1.7a) with Σ_Δ. The results just mentioned above and the analyzed solution of the AHS model strongly suggest that the variety (1.7a) is continuous and that the latter's border represents the coexistence line in the GMSA natural space. Consequently, from the knowledge of Σ_Δ and Σ_χ we can only get some bounds on the regions of existence of the fluid phase, in the sense that the physically allowed parameter region must be smaller than the one bounded by Σ_χ, which in turn is smaller than the one bounded by Σ_Δ. In the same way, one expects that the parameter region where an accurate approximation or even the exact integral equation for the two-point translationally invariant CF does not admit solution[28] is larger that the former ones and smaller than the region where the equation for the one-particle density admits nonuniform solutions.[29,30]

VI. CONCLUSIONS

Over the recent past years, in studying the GMSA, the emphasis shifted toward the approximation of the potential. This point of view limits severely and unnecessarily the usefulness of the method. Besides, it gives more importance to the surface Σ_Δ than appears physically sensible. We hope that this conclusion appears clear or at least reasonable, from the discussion carried through in this paper. In fact, the behavior of the GMSA in the critical region looks quite sound due to the tangency property of Σ_Δ and of Σ_χ. However, the exact critical behavior can never come out from a truncated Dirichlet approximation of the DCF, since this approximation is unable to reproduce the branch point which, according to the general theory of the second-order phase transition, must be present in the FT of the DCF.[20] The fact that Σ_χ lies below Σ_Δ is also interesting, since it may be taken as an indication of the easy access to the region of the metastable states. In other words, the meeting with the coexistence line is not due to the core effects, as described by the GMSA, but is due either to the fact that c_{ext} ceases to make sense—as indicated by the AHS model solution—or, more likely, to the fact that fluctuations, at the level of one-particle functions, can no longer be neglected.

The minimum η_0 in $\kappa_0(\eta)$ is worth a final mention. On the one hand, the existence of the former η_0 appears reasonable, since the GMSA accounts for a balance between attractive and repulsive forces. On the other hand, an accurate GMSA is possible for any potential and in fact any point on the η axis can be a critical point. Consequently, the critical density η_c of a real fluid need not be necessarily equal to η_0. The latter value, however, requires the least attraction, and for that reason we concluded that it has more chance of being met in nature as, indeed, it seems to happen.

ACKNOWLEDGMENT

Partial financial support from the Italian Ministry of Public Instruction is gratefully acknowledged.

APPENDIX A

We report the definitions of the quantitites introduced in Sec. III,

$$a_{\text{PY}} \equiv (1+2\eta)/(1-\eta)^2 , \tag{A1a}$$

$$b_{\text{PY}} \equiv -3\eta/2(1-\eta)^2 , \tag{A1b}$$

and

$$Y \equiv \zeta - a_{\text{PY}} S - b_{\text{PY}} T \tag{A2a}$$

$$= \zeta - [6\eta/\zeta^2(1-\eta)] \times [2-\zeta^2-2(1+\zeta)\exp(-\zeta)] - \Xi , \tag{A2b}$$

where the following definitions have been used:

$$S \equiv (12\eta/\zeta^2)[1-\zeta^2/2-(1+\zeta)\exp(-\zeta)] , \tag{A3a}$$

$$T \equiv (12\eta/\zeta)[1-\zeta-\exp(-\zeta)] , \tag{A3b}$$

$$\Xi \equiv [18\eta^2/\zeta^2(1-\eta)^2][2-\zeta-(2+\zeta)\exp(-\zeta)] . \tag{A3c}$$

Quantities X, E, and F are given by

$$X \equiv 6\eta\{\zeta\exp(-\zeta) - [6\eta/\zeta^2(1-\eta)] \times [2-2\zeta-(2-\zeta^2)\exp(-\zeta)] - \Xi\} , \tag{A4}$$

$$E \equiv -6\eta + \frac{12\eta}{\zeta(1-\eta)^2}(1+2\eta-6\eta/\zeta)S - \frac{12\eta}{\zeta(1-\eta)^2}[3\eta/2+(1-4\eta)/\zeta]T , \tag{A5}$$

$$F \equiv \frac{12\eta}{\zeta(1-\eta)^2}(F_1 S - F_2 T) + F_3 , \tag{A6}$$

while F_1, F_2, and F_3 are defined in the following way:

$$F_1 \equiv f_1(\eta,\zeta)[1-(1+\zeta)\exp(-\zeta)] + 3\eta\zeta\exp(-\zeta) , \tag{A7a}$$

$$F_2 \equiv f_2(\eta,\zeta)[1-(1+\zeta)\exp(-\zeta)] - [(1-4\eta)/2]\zeta\exp(-\zeta) , \tag{A7b}$$

$$F_3 \equiv -6\eta[1-\exp(-\zeta)]^2 \tag{A7c}$$

with

$$f_1(\eta,\zeta) \equiv 1+2\eta-6\eta/\zeta \tag{A7d}$$

and

$$f_2(\eta,\zeta) \equiv 3\eta/2+(1-4\eta)/\zeta . \tag{A7e}$$

Besides the former definitions, which are essentially the Cummings-Smith[12] ones, it will be useful to know that $E-F$ can be written as

$$E-F=\exp(-\zeta)\left[-6\eta[2-\exp(-\zeta)]+\frac{12\eta}{\zeta(1-\eta)^2}(Se_S-Te_T)\right], \quad \text{(A8)}$$

where

$$e_S\equiv\zeta(1-\eta)+(1-4\eta)-\frac{6\eta}{\zeta}$$

and (A9)

$$e_T\equiv\frac{1-\eta}{2}\zeta+\frac{2-5\eta}{2}+\frac{1-4\eta}{\zeta}\ .$$

Finally, the quantity r, defined by Eq. (4.4a), is given by

$$r\equiv\frac{X}{(6\eta)^2}-\frac{Y}{6\eta}\ . \quad \text{(A10)}$$

We report the leading asymptotic expansions at *large* ζ of some quantities which are referred to in the paper. From Eq. (A4) one finds

$$X\approx 36\eta^2\left[\frac{2+\eta}{(1-\eta)^2\zeta}-\frac{2(1+2\eta)}{(1-\eta)^2\zeta^2}\right]+O(\zeta^2\exp(-\zeta))\ , \quad \text{(A11)}$$

while from Eq. (A2) one gets

$$Y\approx\zeta+\frac{6\eta}{1-\eta}+\frac{18\eta^2}{(1-\eta)^2\zeta}+O(\zeta^{-2})\ . \quad \text{(A12)}$$

From the definitions (4.11) one gets

$$A_1\approx\zeta+o,\quad A_2\approx\frac{12\eta(1-\eta)}{1+2\eta}\zeta+o\ . \quad \text{(A13)}$$

From the definition (4.14) and from (A13) one obtains

$$B_0\approx\left[\frac{12\eta(1-\eta)}{1+2\eta}\zeta\right]^2+O(\zeta)\ ,$$
$$B_1\approx O(\zeta),\quad B_1\approx-\zeta^2+O(\zeta)\ . \quad \text{(A14)}$$

Using these results, from Eq. (4.13) it follows that

$$\delta_\chi^{\pm}\approx\pm\frac{1+2\eta}{12\eta(1-\eta)}+o\ . \quad \text{(A15)}$$

For the sake of making the derivation of our analysis easier, we report some intermediate algebraic results concerning the asymptotic expansion of some quantities at *small* ζ. In particular, these are

$$F_1\approx\frac{\zeta^2}{2}-\frac{4-\eta}{12}\zeta^3+\frac{(5-2\eta)\zeta^4}{40}+o\ , \quad \text{(A16a)}$$

$$F_2\approx\frac{(2+\eta)\zeta^2}{12}-\frac{\zeta^3}{8}+\frac{(4-\eta)\zeta^4}{80}+o\ , \quad \text{(A16b)}$$

$$F\approx-\frac{6\eta\zeta^2}{(1-\eta)^2}+\frac{6\eta\zeta^3}{(1-\eta)^2}-\left[\frac{7}{2}-\frac{\eta}{5}\right]\frac{6\eta\zeta^4}{(1-\eta)^2}+o\ , \quad \text{(A17)}$$

$$E/F\approx-\frac{12\eta}{\zeta^3}\left[1+\frac{\zeta}{8b_{\rm PY}}+\zeta^2\left[\frac{1}{8b_{\rm PY}}+\frac{\eta}{10}-\frac{1}{4}\right]+O(\zeta^3)\right]\ , \quad \text{(A18)}$$

$$Y\approx a_{\rm PY}\zeta+b_{\rm PY}\zeta^2+\frac{6\eta(8+\eta)}{120(1-\eta)^2}\zeta^3-\frac{10+2\eta}{720(1-\eta)^2}\zeta^4+o\ , \quad \text{(A19)}$$

and

$$\frac{X}{36\eta^2}-\frac{Y}{6\eta}\equiv r\approx-\frac{\zeta}{6\eta(1-\eta)}+\frac{\zeta^2}{12\eta(1-\eta)}-\frac{10-\eta}{60\eta(1-\eta)}\zeta^3+o\ . \quad \text{(A20)}$$

APPENDIX B

In order to analyze the behavior of $a(K,\zeta,\eta)$ as $K\approx\kappa_0(\eta)\zeta^{\varpi}$ and $\zeta\to 0$ the knowledge of the physical root of the quartic equation (3.5) is required. By combining the former limits and the *small* ζ limiting behavior of X and Y resulting from Eqs. (A19) and (A20) we obtain that the coefficients of Eq. (3.5) have the following *small-*ζ behavior:

$$K^2\sim\kappa_0^2(\eta)\zeta^{2\varpi}+o\ ,$$
$$KY\sim\kappa_0(\eta)a_{\rm PY}\zeta^{\varpi+1}+o\ , \quad \text{(B1)}$$
$$X\sim\frac{18\eta^2}{(1-\eta)^2}\zeta+o\ .$$

Standard Newton analysis yields that the four roots behave as

$$\sim\zeta,\quad\sim\zeta^{(2\varpi-1)/3},\quad\sim\zeta^{\varpi/2},\quad\sim\zeta^{\varpi-1}\ . \quad \text{(B2)}$$

The physical root, however, is the last one and corresponds to $\delta_f=K/Y+o$. In fact, it is the smallest one and has the right virial limit.

When $\varpi=2$ the former four roots behave exactly in the same way and a further analysis is required in order to isolate the physical one. To this aim we set

$$\delta=\tau\zeta/\sqrt{6\eta}$$

in Eq. (3.5) and then we divide by ζ^4. By using, once more, the small-ζ asymptotic behaviors (B1), the quartic equation (3.5) becomes

$$(\tau^2+\kappa^2)(\tau^2-a_{\rm PY}\tau/\sqrt{6\eta}+\kappa)+o=0\ .$$

The solutions are easily obtained and the physical solution turns out to be

$$\delta_f=\frac{a_{\rm PY}[1-(1-24\eta\kappa/a_{\rm PY}^2)^{1/2}]}{12\eta}\zeta+o$$
$$\equiv\frac{a_{\rm PY}r_a(\eta)}{12\eta}\zeta+o\ . \quad \text{(B3)}$$

By combining these results with the small-ζ expansions, reported in the final part of Appendix A, and, of course,

by some algebraic manipulations, one obtains Eq. (4.18), i.e., the leading term in the small-ζ expansion of $a(\eta,K,\zeta)$.

For the reader's greater convenience, we report here some intermediate steps in the derivation of the aforesaid results.

We found it convenient to write Eq. (3.7) as

$$\Delta a \equiv a - a_{\rm PY} = -8b_{\rm PY}(\mathcal{A}_1+\mathcal{A}_2-\mathcal{A}_3) , \tag{B4}$$

with

$$\mathcal{A}_1 \equiv \frac{\delta\exp(\zeta)}{\zeta}\left[\frac{E(\eta,\zeta)F_1(\eta,\zeta)}{F(\eta,\zeta)}-f_1(\eta,\zeta)\right] \equiv \frac{\delta\exp(\zeta)}{\zeta}\overline{\mathcal{A}}_1 , \tag{B5a}$$

$$\mathcal{A}_2 \equiv \frac{F_1 Y}{F\zeta} , \tag{B5b}$$

and

$$\mathcal{A}_3 \equiv \frac{K}{\delta}\frac{F_1}{\zeta F} \equiv \frac{K}{\delta}\overline{\mathcal{A}}_3 . \tag{B5c}$$

By using Eqs. (A18), (A19), and (A16a) one obtains

$$\overline{\mathcal{A}}_1 \approx -\frac{(1-\eta)^2}{2}+\frac{(1-\eta)^2(6+\eta)}{12}\zeta+O(\zeta^2) ,$$

$$\mathcal{A}_2 \approx \frac{a_{\rm PY}}{8b_{\rm PY}}+O(\zeta) ,$$

$$\overline{\mathcal{A}}_3 \approx \frac{1}{8\zeta b_{\rm PY}}\left[1+\zeta\frac{\eta-2}{6}+\frac{\eta\zeta^2}{5}\right]+O(\zeta^2) .$$

From the latter results, by using the fact that $\delta_f \approx K/Y \approx \kappa(\eta)\zeta^{\varpi-1}/a_{\rm PY}$, when $\varpi>2$, one finds that

$$\mathcal{A}_1-\mathcal{A}_3 \to -\frac{a_{\rm PY}}{8b_{\rm PY}}$$

and Eq. (4.18) follows.

When $\varpi=2$, one finds that

$$\mathcal{A}_1-\mathcal{A}_3 \to -\frac{1}{16b_{\rm PY}a_{\rm PY}r_a(\eta)}[24\eta\kappa(\eta)-a_{\rm PY}^2 r_a^2(\eta)]$$

and Eq. (4.19a) is proved.

In the following we shall need the asymptotic behavior of $b(\eta,\zeta,k)$ in the case $\varpi=2$. In order to evaluate it, we note that from Eqs. (3.8) and (A7e) it follows that

$$\Delta b \equiv b-b_{\rm PY} = \frac{8b_{\rm PY}\delta_f\exp(\zeta)}{\zeta}[d(\eta,\zeta,K)F_2(\eta,\zeta)-f_2(\eta,\zeta)] , \tag{B6}$$

while d, defined by Eq. (3.6), can be written as

$$d = \frac{(36\eta^2\delta_f^2 - X\delta_f+12\eta K)\exp(-\zeta)}{KF}+E/F \tag{B7}$$

after having used Eq. (3.5). Recalling now that near the critical point $r_a(\eta)=1$ by Eqs. (4.21) and (4.19b), Eqs. (B1a) and (B3) become

$$K \approx \kappa_0(\eta)\zeta^2+o , \tag{B8a}$$

$$\delta_f \approx \frac{a_{\rm PY}\zeta}{12\eta}+o . \tag{B8b}$$

By using Eqs. (A17) and (A18), it is easy to show that

$$d \approx -12\eta/\zeta^3+O(\zeta^{-2}) \tag{B8c}$$

and then, from Eq. (B6), by Eqs. (A16b) and (A7c), that

$$b \approx 12\eta\delta_f/\zeta^2+o(\zeta^{-1}) \approx a_{\rm PY}(\eta)/\zeta+o(\zeta^{-1}) . \tag{B8d}$$

APPENDIX C

The behavior of the correlation length of the CF at the critical point is now worked out in the one-Yukawa GMSA. The FT of OZ relation yields

$$\tilde{h}(z,\eta,\zeta,K) = \frac{\tilde{c}(z,\eta,\zeta,K)}{1-p\tilde{c}(z,\eta,\zeta,K)} \equiv \frac{\tilde{c}(z,\eta,\zeta,K)}{\mathcal{D}(z,\eta,\zeta,K)} , \tag{C1}$$

where $\tilde{c}(z,\eta,\zeta,K)$ represents the analytic continuation of the FT of $c(r,\eta,\zeta,K)$. Moreover, the GMSA's necessarily yield meromorphic $\tilde{c}(z,\dots)$'s. The large-r asymptotic behavior of the CF is determined by the zero of $\mathcal{D}(z,\eta,\zeta,K)$ closest to the origin. Thus we have to expand $\tilde{c}(z,\dots)$ at small z's. From Eqs. (2.8) and (2.8a) one immediately gets

$$\mathcal{D}(z,\eta,\zeta,K) \approx \tilde{Q}^2(0)+z^2(\tilde{Q}_2\tilde{Q}(0)-\tilde{Q}_1^2)+O(z^4) , \tag{C2}$$

where

$$\tilde{Q}_1 \equiv -12\eta i\int_0^\infty r\exp(ikr)Q(r)dr\,|_{k=0} \equiv -12\eta i q_1 , \tag{C3}$$

$$\tilde{Q}_2 \equiv 12\eta\int_0^\infty r^2 Q(r)dr \equiv 12\eta q_2 . \tag{C4}$$

Using Eq. (3.2) with $N=1$ and the definitions (3.4), one obtains

$$q_1 = -a/8-b/6+\delta\exp(\zeta)/\zeta^2 + d\delta[1+\zeta+\zeta^2/2-\exp(\zeta)]/\zeta^2 \tag{C5}$$

and

$$q_2 = -a/15-b/12+2\delta\exp(\zeta)/\zeta^3 + 2d\delta[1+\zeta+\zeta^2/2+\zeta^3/6-\exp(\zeta)]/\zeta^3 . \tag{C6}$$

The knowledge of the leading asymptotic term for the quantities present on the rhs of Eqs. (C5) and (C6), i.e., Eqs. (4.19a), (B8a), (B8c), and (B8d), immediately yields

$$q_1 \approx \frac{a_{\rm PY}(1-2\eta)}{12\eta\zeta}+o(\zeta^{-1}) , \tag{C7a}$$

$$q_2 \approx \frac{a_{\rm PY}}{6\eta\zeta^2}+O(\zeta^{-1}) . \tag{C7b}$$

Substituting in Eq. (C2), recalling Eq. (3.9) as well as that

$$a(\eta,\zeta) \approx a_1(\eta)\zeta+o$$

with $a_1(\eta)$ an unknown η function, one finds that

$$\mathcal{D}(z,\ldots)\approx a_1^2(\eta)\zeta^2+z^2\left[\frac{a_{\mathrm{PY}}(1-2\eta)}{\zeta}\right]^2+o\ . \tag{C8}$$

We recall now that

$$h(r,\ldots)=(4\pi/r)\int_0^\infty k\sin(kr)\tilde{h}(k,\ldots)dk$$
$$=(2\pi/r)\mathcal{F}\left[\int_{-\infty}^{\infty}k\exp(ikr)\tilde{h}(k,\ldots)dk\right]\ .$$

The use of the residue theorem and Eq. (C8) allow us to get

$$h(r,\ldots)\approx\frac{\pi^3\zeta^2}{3\eta_c a_{\mathrm{PY}}^2(1-2\eta)^2}\times\frac{\exp[-|a_1(\eta)|\zeta^2 r/a_{\mathrm{PY}}(1-2\eta)]}{r}\ ,$$
$$r\gg 1\ . \tag{C9'}$$

This relation proves that the inverse correlation length of the CF is $O(\zeta^2)$. Moreover, at the critical point, Eq. (C9') predicts that $h(r,\ldots)\to 0$. We think that this result is only a caricatural attempt of the GMSA to reproduce a CF which decreases faster than r^{-1}. Finally, the singularity present as $\eta\to\frac{1}{2}$ cannot be taken seriously, since it only indicates that in Eqs. (C7) we have to account for the next-higher-order terms.

APPENDIX D

Since

$$K\approx\frac{\lambda\zeta}{12}\ , \tag{D1}$$

the asymptotic behaviors of the coefficients of the quartic equation (3.5) follow immediately from Eqs. (A11) and (A12). In this way one finds that the physical root behaves as

$$\delta_f\approx\frac{K}{Y}\approx\frac{\lambda}{12}+O(\zeta^{-1})\ . \tag{D2}$$

Equations (5.16) and (5.17) have been obtained by evaluating the limits of (3.7) and (3.8) as $\zeta\to\infty$, knowing that Eqs. (D1) and (D2) hold true. This job becomes rather easy once one notices that

$$d-1=\exp(-\zeta)[-K+\delta Y+R(\eta,\zeta)]\ ,$$

where $R(\eta,\zeta)$ denotes the expression inside square brackets on the RHS of Eq. (A8). Algebraic manipulations yield

$$a=a_{\mathrm{PY}}-\frac{8b_{\mathrm{PY}}\delta}{\zeta}\left[f_1\left[\frac{R+\delta Y-K}{F\delta^2}-d(1+\zeta)\right]+3\eta\zeta d\right]\ ,$$

$$b=b_{\mathrm{PY}}+\frac{8b_{\mathrm{PY}}\delta}{\zeta}\left[\left[\frac{3\eta}{2}+\frac{1-4\eta}{\zeta}\right]\times\left[\frac{R+\delta Y-K}{F\delta^2}-d(1+\zeta)\right]-\frac{1-4\eta}{2}\zeta d\right]\ .$$

By using the fact that at large ζ,

$$R(\zeta,\eta)\approx-12\eta+O(\zeta^{-1})\ , \tag{D3}$$

$$d\approx 1+O(\exp(-\zeta))\ , \tag{D4}$$

Equations (5.16) and (5.17) follow quite easily and almost immediately. Moreover, from Eqs. (3.4), (D2), and (D4) one finds that

$$c_1\approx-\lambda/12+O(\zeta^{-1})\ . \tag{D5}$$

[1]E. Waisman, Mol. Phys. **25**, 45 (1973).
[2]E. Waisman, J. Chem. Phys. **59**, 495 (1973).
[3]B. Larsen, G. Stell, and K. C. Wu, J. Chem. Phys. **67**, 530 (1977); D. K. Chaturvedi, G. Senatore, and M. P. Tosi, Nuovo Cimento B **62**, 375 (1980).
[4]C. Carraro and S. Ciccariello, Phys. Rev. A **35**, 3472 (1987).
[5]G. Pastore and E. M. Waisman, Mol. Phys. **61**, 849 (1987).
[6]A. L. Kholodenko and A. L. Beyerlein, Phys. Rev. A **34**, 3309 (1986).
[7]P. T. Cummings and G. Stell, J. Chem. Phys. **78**, 1917 (1983).
[8]J. Konior and C. Jedrzejek, Mol. Phys. **48**, 219 (1983).
[9]J. S. Høye, G. Stell, and E. Waisman, Mol. Phys. **32**, 209 (1976).
[10]J. S. Høye and G. Stell, Mol. Phys. **25**, 195 (1976).
[11]J. S. Høye and L. Blum, J. Stat. Phys. **16**, 399 (1976).
[12]P. T. Cummings and E. R. Smith, Mol. Phys. **38**, 997 (1979).
[13]J. S. Høye and G. Stell, Mol. Phys. **52**, 1057 (1984).
[14]L. Schwartz, *Etudes des Sommes d'Exponentielles*, (Hermann, Paris, 1959), pp. 10–12.
[15]A. Munster, *Statistical Thermodynamics* (Springer-Verlag, Berlin, 1969), Vol. I, pp. 532–536.
[16]R. J. Baxter, in *Physical-Chemistry, An Advanced Treatise: Liquid State*, edited by H. Eyring, H. Henderson, and W. Jost (Academic, New York, 1971), Vol. 8A, p. 267.
[17]We note that the quantities K, c, and d, used by Høye and Blum, must be written as $K_i\exp(z_i)$, etc., in order to have our K, c, and d.
[18]It is likely that the same conclusion holds true even in the two-Yukawa case. In fact, we have numerically explored the relative configuration of the two surfaces by using the parametrizations reported in Ref. 8. Although the number of considered cases has not been large, we always found Σ_γ below Σ_Δ, quite similarly to the figures shown in Ref. 8.
[19]M. J. Green, J. Chem. Phys. **33**, 1403 (1960).
[20]M. Fisher, J. Math. Phys. **5**, 944 (1964) [see also M. Fisher, in *Critical Phenomena, Proceedings of the Conference*, Vol. 186 of *Lecture Notes in Physics*, edited by F. J. Hahne (Springer-Verlag, Berlin, 1983)]; A. M. Polyakov, Zh. Eksp. Teor. Fiz.

55, 1026 (1968) [Sov. Phys.—JETP **28**, 533 (1969)].

[21]In order to avoid possible confusion, we have added an overbar to the standard definition of the critical indices, reported in Ref. 22.

[22]E. H. Stanley, *Introduction to Phase Transitions and Critical Phenomena* (Oxford Universtiy Press, New York, 1971).

[23]This limiting situation looks quite similar to that analyzed by Kac, Uhlenbeck, and Hemmer, (Ref. 24) with the important difference that in our case it is applied to the DCF and not to the interaction. Besides we recall that Høye and Stell in the last section of Ref. 10 have noted the importance of this limit and after a brief discussion they erroneously concluded that the behavior is the mean-field one.

[24]M. Kac, G. E. Uhlenbeck, and P. C. Hemmer, J. Math. Phys. **4**, 216 (1963); **5**, 60 (1964).

[25]J. O. Hirschfelder, C. F. Curtiss, and R. B. Bird, *Molecular Theory of Gases and Liquids* (Wiley, New York, 1954).

[26]By contrast, from Eq. (4.15), one sees that K_χ^+ increases with ζ and thus it happens that at small densities, i.e., $\eta < \eta_c = 0.121$, the quantity $12K_\chi^+/\zeta$ turns out larger than $12K_{\rm AHS}(\eta,\zeta)/\zeta = \lambda(\eta,\tau)$, while when $\eta > \eta_c$, $12K_\chi^+/\zeta$ becomes smaller than $12K_{\rm AHS}(\eta,\zeta)/\zeta$. We note that these quantities correspond, respectively, to the dotted and to the dashed lines of Fig. 12 in Ref. 16.

[27]It might be interesting to know that the values of K and ζ resulting from Fig. 2 of Ref. 4 at the HS packing fraction value $\eta_f = 0.494$ are, respectively, 1.39 and 29.3. The corresponding K_χ^+ and K_Δ^+ values are 22.26 and 46.23. One understands how far the former GMSA point is from the characteristic GMSA surfaces.

[28]P. D. Poll And N. W. Ashcroft, Phys. Rev. A **35**, 5167 (1987); G. A. Martynov and G. N. Sarkisov, Mol. Phys. **49**, 1495 (1983).

[29]J. K. Percus, in *The Liquid State of Matter*, edited by E. W. Montroll and J. L. Lebowitz (North-Holland, Amsterdam, 1982).

[30]R. Lovett, J. Chem. Phys. **88**, 7739 (1988).